Spin Exchange Coupling in Heterobimetallic $M^{II}V^{IV}O$ (M = Cu, Ni, Co, Fe, Mn) Macrocyclic Complexes. Synthesis, Structure, and Properties

Sasankasekhar Mohanta,[†] Kausik K. Nanda,[†] Laurence K. Thompson,[‡] Ulrich Flörke,[§] and Kamalaksha Nag*,[†]

Department of Inorganic Chemistry, Indian Association for the Cultivation of Science, Calcutta 700 032, India, Department of Chemistry, Memorial University of Newfoundland, St. John's, Newfoundland, Canada A1B 3X7, and Anorganische und Analytische Chemie der Universität Gesamthochschule Paderborn, D-33098 Paderborn, Germany

Received September 13, 1997

A series of heterobimetallic complexes $[(V^{IV}O)L1Cu^{II}(\mu\text{-OAC})(MeOH)](ClO_4)$ (**1**) and $[(V^{IV}O)L1M^{II}(\mu\text{-OAc})(H_2O)](ClO_4)\cdot H_2O$ (M = Ni (**2**), Co (**3**), Fe (**4**), Mn (**5**)) derived from a symmetric tetraaminodiphenol macrocyclic ligand H_2L1 have been synthesized and characterized. The crystal structure of **1** has been determined. The complex ($C_{27}H_{41}N_4O_{10}ClCuV$) crystallizes in the monoclinic space group $P2_1/c$ with $a = 13.227(3)$ Å, $b = 14.932(3)$ Å, $c = 17.019(3)$ Å, $\beta = 112.29(1)°$, and $Z = 4$. Both the metal centers in **1** are six-coordinated and are triply bridged by the two phenolate and the acetate oxygens; the sixth coordination site of the copper atom is occupied by a distantly placed methanol oxygen (Cu−O = 2.452(5) Å), while that of the vanadium by the oxo oxygen (V−O = 1.627(4) Å). The metal centers are separated by 3.066(1) Å, and the dihedral angle (Δ) between the metal planes is 32.0°. Variable-temperature (4−300 K) magnetic susceptibility measurements of **1**−**5** and of $[(V^{IV}O)L2Cu^{II}(\mu\text{-OAc})(H_2O)](ClO_4)$ (**6**) (where H_2L2 is an asymmetric tetraaminodiphenol macrocyclic ligand) have been made and treated with the spin-Hamiltonian $\mathbf{H} = -2J\mathbf{S}_1\cdot\mathbf{S}_2$. All the complexes, except **5**, exhibit ferromagnetic exchange interaction with the following values of J (in cm^{-1}): 42.5 (**1**), 12.0 (**2**), 4.4 (**3**), 4.4 (**4**), and 46.0 (**6**); complex **5** behaves antiferromagnetically with $J = -14.2$ cm^{-1}. A linear correlation between J and Δ has been proposed for $Cu^{II}V^{IV}O$ complexes.

Introduction

The intimate relationship between spin coupling and molecular structure has fostered the emergence of molecular magnetism[1] as a multidisciplinary field of research.[2,3] The dissection of spin exchange interactions into ferromagnetic and antiferromagnetic components and identification of these with specific orbital interactions[1,4,5] have stimulated quantitative calculation[6] of magnetic coupling constants as well as to obtain empiric magnetostructural correlations.[7−12]

Although numerous binuclear metal complexes have been studied structurally and magnetically, only a small fraction of them (less than 5%) are estimated[13] to exhibit overall ferromagnetic behavior. The designing of molecular system that would spontaneously order below a certain critical temperature to display a zero-field magnetization is considered as a major challenging task. One of the strategies to obtain molecular magnet is to induce parallel alignment of neighboring spins through self-assembly of ferromagnetically coupled heterobi-

[†] Indian Association for the Cultivation of Science.
[‡] Memorial University of Newfoundland.
[§] Universität Gesamthochschule Paderborn.

(1) Kahn, O. *Molecular Magnetism*; VCH Publications: New York, 1993.
(2) O'Connor, C. J. Ed.; *Research Frontiers in Magnetochemistry*; World Scientific: Singapore, 1993.
(3) Gatteschi, D., Kahn, O., Miller, J. S., Palacio, F., Eds.; *Magnetic Molecular Materials*; Kluwer Academic Publishers: Dordrecht, The Netherlands, 1991.
(4) (a) Goodenough, J. B. *J. Phys. Chem. Solids* **1958**, *6*, 287. (b) Kanamori, J. *J. Phys. Chem. Solids* **1959**, *10*, 87. (c) Ginsberg, A. P. *Inorg. Chim. Acta Rev.* **1971**, *5*, 45.
(5) (a) Hay, P. J.; Thibeault, J. C.; Hoffman, R. *J. Am. Chem. Soc.* **1975**, *97*, 4884. (b) Girerd, J. J.; Charlot, M. F.; Kahn, O. *Mol. Phys.* **1977**, *34*, 1063. (c) Kahn, O. *Angew. Chem., Int. Ed. Engl.* **1985**, *24*, 834.
(6) For example, see: (a) Ruiz, E.; Alemany, P.; Alvarez, S.; Cane, J. *J. Am. Chem. Soc.* **1997**, *119*, 1297. (b) Baron, V.; Gillon, B.; Cousson, A.; Mathoniere, C.; Kahn, O.; Grand, A.; Ohrstrom, L.; Delley, B.; Bonnet, M.; Boucherle, J. X. *J. Am. Chem. Soc.* **1997**, *119*, 3500. (c) Wang, C.; Fink, K.; Staemmler, V. *Chem. Phys.* **1995**, *192*, 25. (d) Noodleman, L.; Peng, C. Y.; Case, D. A.; Mouesca, J. M. *Coord. Chem. Rev.* **1995**, *144*, 199. (e) Schmitt, E. A.; Noodleman, L.; Baerends, E. J.; Hendrickson, D. N. *J. Am. Chem. Soc.* **1992**, *114*, 4, 6109. (f) de Loth, P.; Karafiloglou, P.; Daudey, J. P.; Kahn, O. *J. Am. Chem. Soc.* **1988**, *110*, 5676. (g) Albonico, C.; Bencini, A.; *Inorg. Chem.* **1988**, *27*, 1934. (h) Astheimer, H.; Haase, W. *J. Chem. Phys.* **1986**, *85*, 1427.
(7) Willet, R. D., Gatteschi, D., Kahn, O., Eds.; *Magneto-Structural Coorelations in Exchange Coupled Systems*; Kluwer Academic Publishers: Dordrecht, The Netherlands, 1985.
(8) (a) Crawford, V. M.; Richaradson, M. W.; Wasson, J. R.; Hodgson, D. J.; Hatfield, W. E. *Inorg. Chem.* **1976**, *15*, 2107. (b) Merz, L.; Haase, W. *J. Chem. Soc., Dalton Trans.* **1980**, 875. (c) Charlot, M. F.; Kahn, O.; Jeanin, S.; Jeanin, Y. *Inorg. Chem.* **1980**, *19*, 1410. (d) Thompson, L. K.; Mandal, S. K.; Tandon S. S.; Bridson, J. N.; Park, M. K. *Inorg. Chem.* **1996**, *35*, 3117.
(9) (a) Nanda, K. K.; Thompson, L. K.; Bridson, J. N.; Nag, K. *J. Chem. Soc., Chem. Commun.* **1994**, 1337. (b) Ribas, J.; Monfort, M.; Diaz. C.; Bastos, C.; Solans, X. *Inorg. Chem.* **1993**, *32*, 3557. (c) Escuer, A.; Vicente, R.; Ribas, J.; El Fallah, M. S.; Solans, X.; Font-Bardia, M. *Inorg. Chem.* **1993**, *32*, 3727.
(10) Gorun, S. M.; Lippard, S. J. *Inorg. Chem.* **1991**, *30*, 1625.
(11) (a) Glerup, J.; Hodgson, D. J.; Pederson, E. *Acta Chem. Scand.* **1983**, *A37*, 161. (b) Niemann, A.; Bossek, U.; Wieghardt, K.; Butzlaff, C.; Trautwein, A. X.; Nuber, B. *Angew. Chem., Int. Ed. Engl.* **1992**, *31*, 311. (c) Spiccia, L.; Fallon, G. D.; Markiewicz, A.; Murray, K. S.; Riesen, H. *Inorg. Chem.* **1992**, *31*, 1066.
(12) Plass, W. *Angew. Chem., Int. Ed. Engl.* **1996**, *35*, 627.
(13) Chen, C. T.; Suslick, K. S. *Coord. Chem. Rev.* **1993**, *128*, 293.

S0020-1669(97)01176-2 CCC: $15.00 © 1998 American Chemical Society
Published on Web 03/10/1998

Chart 1

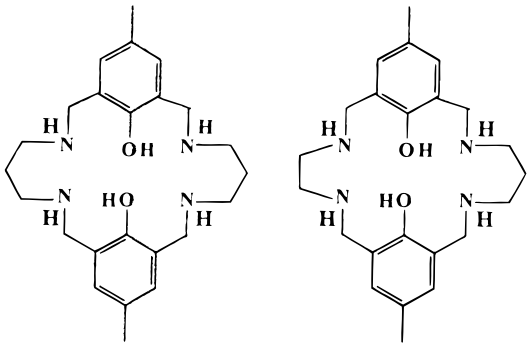

H_2L1 H_2L2

metallic building blocks. Kahn[14] first proposed that a definitive way to obtain ferromagnetically coupled bimetallic systems would be to involve symmetry-related strict orthogonality of the magnetic orbitals of the interacting metal centers. It was demonstrated[15] that in the heterobinuclear $Cu^{IV}V^{IV}O$ complex [CuVO{$(fsa)_2$-en}(MeOH)] (where {$(fsa)_2$-en} is *N*,*N*′-bis(2-hydroxy-3-carboxybenzylidene)-1,2-diaminoethane) the triplet ground state is separated from the less populated singlet state by 118 cm^{-1}. Subsequently, this concept has been used to produce ferromagnetic effect in several other systems, viz. $Cu^{II}{}_2V^{IV}O$,[16] $Cu^{II}Cr^{III}$,[17,18] $Cu^{II}Mn^{III}$,[18] $Ni^{II}{}_3Cr^{III}$,[19] and $Ni^{II}V^{IV}O$.[20]

In the course of our studies on magnetostructural relationships in metal complexes of the tetraaminodiphenol macrocyclic ligands H_2L1 and H_2L2 (Chart 1), we have examined several types of homo- and heterobinuclear systems,[91,20,21] including the carboxylate-bridged complexes.[22] The present study is concerned with the structural characterization, electrochemical behavior and magnetic properties of the heterobinuclear complexes $[Cu^{II}V^{IV}OL1(\mu\text{-OAc})(MeOH)](ClO_4)$ (**1**), $[M^{II}V^{IV}OL1(\mu\text{-OAc})(H_2O)](ClO_4).H_2O$ (M = Ni, Co, Fe, Mn) (**2**−**5**), and $[Cu^{II}V^{IV}OL2(\mu\text{-OAc})(H_2O)]\cdot H_2O$ (**6**). Although magnetic exchange interactions in the heterobimetallic $Cu^{II}M^{II}$ (M = Ni, Co, Fe, Mn) complexes of related tetraiminodiphenol macrocyclic have been investigated,[23] to our knowledge there is no reported study on the $M^{II}V^{IV}O$ series with any binucleating ligand.

Experimental Section

Physical Measurements. Infrared spectra were recorded on a Perkin-Elmer 783 spectrophotometer using KBr disks. Electronic absorption spectra were obtained with Shimadzu UV 2100 and Hitachi U3400 spectrophotometers over the UV−vis and near-IR regions. Cyclic voltammetric and differential pulse voltammetric measurements were carried out at room temperature in acetonitrile or dimethyl sulfoxide solutions (ca. 1 mM) under N_2 using a BAS 100B electrochemical analyzer (Bioanalytical Systems Inc.). The supporting electrolyte was tetraethylammonium perchlorate (TEAP, 0.1 M). A three-electrode assembly (BAS) comprising a glassy-carbon or platinum disk working electrode, a platinum auxiliary electrode, and a Ag/AgCl reference electrode were used. The reference electrode was separated from the bulk solution with a salt bridge having Vycor plug. IR compensation was achieved before each CV was recorded. The ferrocene/ferrocenium couple was used to monitor the reference electrode and was observed at 0.36 V. Elemental (C, H, and N) analyses were performed on a Perkin-Elmer 2400II analyzer.

Variable-temperature magnetic susceptibility data of the powdered samples were measured in the range 4−300 K by using an Oxford Instruments superconducting Faraday magnetic susceptibility system with a Sartorius 4432 microbalance. A main solenoid field of 1.5 T and a gradient field of 10 T m^{-1} were employed. Susceptibility data were corrected for diamagnetism (Pascal corrections), for temperature-independent paramagnetism (TIP), and for the presence of monomeric impurity. $Hg[Co(NCS)_4]$ was used as a calibration standard.

Synthesis. The macrocyclic ligands H_2L1[24] and H_2L2[21c] and the oxovanadium(IV) complex $[VOL1]\cdot H_2O$[20b] were prepared as reported earlier.

Caution: *The perchlorate salts of the metal complexes described below may be explosive and should be handled with great care!*

$[(V^{IV}O)L1Cu^{II}(\mu\text{-OAC})(MeOH)](ClO_4)$ (1), $[(V^{IV}O)L1Ni^{II}(\mu\text{-OAc})(H_2O)](ClO_4)\cdot H_2O$ (2), $[(V^{IV}O)L1Co^{II}(\mu\text{-OAc})(H_2O)](ClO_4)\cdot H_2O$ (3), $[(V^{IV}O)L1Fe^{II}(\mu\text{-OAc})(H_2O)](ClO_4)\cdot H_2O$ (4), and $[(V^{IV}O)L1Mn^{II}(\mu\text{-OAc})(H_2O)](ClO_4)\cdot H_2O$ (5). All these complexes were prepared in the same way as illustrated below for **1**, except that $Cu(ClO_4)_2\cdot 6H_2O$ was replaced with appropriate $M(ClO_4)_2\cdot 6H_2O$ (M = Ni, Co, Fe, Mn). The reactions involving the formation of complexes **3**−**5** were carried out under an atmosphere of nitrogen.

To a stirred suspension of $[(V^{IV}O)L1]\cdot H_2O$ (0.49 g, 1 mmol) in methanol (50 mL) at room temperature were added NaOAc (0.16 g, 2 mmol) and $Cu(ClO_4)_2\cdot 6H_2O$ (0.37 g, 1 mmol). In a short while a clear yellowish green solution was obtained, from which eventually a green compound began to separate. After 1 h of stirring, the microcrystalline product that deposited was collected by filtration and washed with methanol. This on recrystallization from acetonitrile−methanol (1:1) mixture gave green crystals of **1**, yield 0.67 g (90%). Anal. Calcd for $C_{27}H_{41}N_4O_{10}ClCuV$: C, 44.32; H, 5.60; N, 7.66. Found: C, 44.14; H, 5.67; N, 7.72. Selected IR data [ν, cm^{-1}]: 3260 m (νNH), 1615 sh (δNH), 1575 s ($\nu_{as}CO_2^-$), 1410 s ($\nu_sCO_2^-$), 1090 s, 630 s (νClO_4^-), 945 s (νV═O). UV−vis data [λ_{max}, nm (ϵ, M^{-1} cm^{-1})] in acetonitrile: 685 (65), 390 (705), 285 sh (7960). μ_{eff}: 2.62μ_B at 300 K.

Data for **2**: pink; yield 85%. Anal. Calcd for $C_{26}H_{41}N_4O_{11}ClNiV$: C, 42.73; H, 5.61; N, 7.67. Found: C, 43.01; H, 5.69; N, 7.61. Selected IR data [ν, cm^{-1}]: 3260 w (νNH), 1610 w (δNH), 1565 s ($\nu_{as}CO_2^-$), 1425 ($\nu_sCO_2^-$), 1110 s, 620 s (νClO_4^-), 935 s (νV═O). UV−vis data

(14) Kahn, O.; Galy, J.; Tola, P.; Coudanne, H. *J. Am. Chem. Soc.* **1978**, *100*, 3931.
(15) Kahn, O.; Galy, J.; Journaux, Y.; Jaud, J.; Morgenstern-Badarau, I. *J. Am. Chem. Soc.* **1982**, *104*, 2165.
(16) Bencini, A.; Benelli, C.; Dei, A.; Gatteschi, D. *Inorg. Chem.* **1985**, *24*, 695.
(17) Journaux, Y.; Kahn, O.; Coudanne, H. *Angew. Chem., Int. Ed. Engl.* **1982**, *21*, *1*, 624.
(18) Birkelbach, F.; Winter, M.; Flörke, U.; Haupt, H. J.; Butzlaff, C.; Lenger, M.; Bill. E.; Trautwein, A. X.; Wieghardt. K.; Chaudhuri, P. *Inorg. Chem.* **1994**, *33*, 3, 3990.
(19) Pei, Y.; Journaux, Y.; Kahn, O. *Inorg. Chem.* **1989**, *28*, 100.
(20) (a) Nanda, K. K.; Mohanta, S.; Ghosh, S.; Mukherjee, M.; Helliwell, M.; Nag, K. *Inorg. Chem.* **1995**, *34*, 2861. (b) Mohanta, S.; Nanda, K. K.; Ghosh, S.; Mukherjee, M.; Helliwell, M.; Nag, K. *J. Chem. Soc., Dalton Trans.* **1996**, 4233.
(21) (a) Nanda, K. K.; Das, R.; Thompson, L. K.; Venkatsubramanian, K.; Paul, P.; Nag, K. *Inorg. Chem.* **1994**, *33*, 1188. (b) Das, R.; Nanda, K. K.; Pal, I.; Baitalik, S.; Nag, K. *Polyhedron* **1994**, *13*, 2639. (c) Nanda, K. K.; Das, R.; Vankatsubramanian, K.; Paul, P.; Nag, K. *J. Chem. Soc., Dalton Trans.* **1993**, 2515. (d) Das, R.; Nanda, K. K.; Mukherjee, A. K.; Mukherjee, M.; Helliwell, M.; Nag, K. *J. Chem. Soc., Dalton Trans.* **1993**, 2241. (e) Das, R.; Nag, K. *Inorg. Chem.* **1991**, *30*, 2831.
(22) (a) Dutta, S. K.; Ensling, J.; Werner, R.; Flörke, U.; Gütlich, P.; Haase, W.; Nag, K. *Angew. Chem., Int. Ed. Engl.* **1997**, *36*, 152. (b) Dutta, S. K.; Werner, R.; Flörke, U.; Mohanta, S.; Nanda, K. K.; Haase, W.; Nag, K. *Inorg. Chem.* **1996**, *35*, 2292. (c) Nanda, K. K.; Das, R.; Thompson, L. K.; Vankatsubramanian, K.; Nag, K. *Inorg. Chem.* **1994**, *33*, 5934.
(23) (a) Okawa, H.; Nishio, J.; Ohba, M.; Tadokoro, M.; Matsumoto, N.; Koikawa, M.; Kida, S.; Fenton, D. *Inorg. Chem.* **1993**, *32*, 2949. (b) Lambert, S. L.; Spiro, C. L.; Gagne, R. R.; Hendrickson, D. N. *Inorg. Chem.* **1982**, *21*, 68. (c) Spiro, C. L. Lambert, S. L.; Smith, T. J.; Duesler, E. N.; Gagne, R. R.; Hendrickson, D. N. *Inorg. Chem.* **1981**, *20*, 1229.
(24) (a) Mandal, S. K.; Nag, K. *J. Org. Chem.* **1986**, *51*, 3900. (b) Mandal, S. K.; Thompson, L. K.; Nag, K.; Charland, J. P.; Gabe, E. J. *Inorg. Chem.* **1987**, *26*, 6, 1391.

Table 1. Crystallographic Data for $[(V^{IV}O)L1Cu^{II}(\mu\text{-OAc})(MeOH)](ClO_4)$ (**1**)

empirical formula	$C_{27}H_{41}N_4O_{10}ClCuV$	Z	4
fw	731.57	λ(Mo Kα), Å	0.71073
space group	$P2_1/c$	μ, cm^{-1}	11.31
a, Å	13.227(3)	ρ_{calcd}, g cm^{-3}	1.562
b, Å	14.932(3)	T, °C	20
c, Å	17.019(3)	$R1^a(I > 2\sigma(I))$	0.063
β, deg	112.29(1)	w$R2^b$ (all data)	0.166
V, $Å^3$	3110.2(11)		

^{a} $R1 = [\sum||F_o| - |F_c||/\sum|F_o|]$. ^{b} w$R2 = [\sum w(F_o^2 - F_c^2)^2/\sum w(F_o^2)^2]^{1/2}$.

[λ_{max}, nm (ϵ, M^{-1} cm^{-1})] in acetonitrile: 1060 (5), 725 (25), 530 (70), 290 (8750). μ_{eff}: 3.71μ_B at 300 K.

Data for **3**: pink; yield 70%. Anal. Calcd for $C_{26}H_{41}N_4O_{11}ClCoV$: C, 42.72; H, 5.61; N, 7.67. Found: C, 42.21; H, 5.71; N, 7.56. Selected IR data [ν, cm^{-1}]: 3270 w (νNH), 1600 w (δNH), 1560 s ($\nu_{as}CO_2^-$), 1425 s ($\nu_sCO_2^-$), 1100 s, 625 s (νClO_4^-), 935 (νV=O). UV−vis data [λ_{max}, nm (ϵ, M^{-1} cm^{-1})] in acetonitrile: 1000 (8), 715 (30), 525 (85), 260 (7800). μ_{eff}: 5.36μ_B at 300 K.

Data for **4**: brown; yield 60%. Anal. Calcd for $C_{26}H_{41}N_4O_{11}ClFeV$: C, 42.90; H, 5.64; N, 7.70. Found: C, 43.32; H, 5.68; N, 7.60. Selected IR data [ν, cm^{-1}]: 3260 w (νNH), 1610 (δNH), 1570 ($\nu_{as}CO_2^-$), 1440 s ($\nu_sCO_2^-$), 1110 s, 625 s (νClO_4^-), 950 (νV=O). UV−vis data [λ_{max}, nm (ϵ, M^{-1} cm^{-1})] in acetonitrile: 1040 (10), 730 sh (85), 535 (60), 290 sh (8050). μ_{eff}: 5.68μ_B at 300 K.

Data for **5**: pink; yield 75%. Anal. Calcd for $C_{26}H_{41}N_4O_{11}ClMnV$: C, 42.95; H, 5.64; N, 7.71. Found: C, 42.74; H, 5.72; N, 7.69. UV−vis data [λ_{max}, nm (ϵ, M^{-1} cm^{-1})] in acetonitrile: 720 (45), 530 (100), 290 (8780). μ_{eff}: 5.95μ_B at 300 K.

$[(V^{IV}O)L2Cu^{II}(\mu\text{-OAc})(H_2O)](ClO_4)\cdot H_2O$ (6). To a stirred methanol solution (50 mL) of H_2L2 (0.79 g, 2 mmol) was added a second methanol solution (25 mL) of $VO(acac)_2$ (0.53 g, 2 mmol) over a period of 30 min. An orange red product that began to deposit was stirred additionally for 1 h. The suspension was then treated successively with NaOAc (0.33 g, 4 mmol) and $Cu(ClO_4)_2\cdot 6H_2O$ (0.74 g, 2 mmol), and stirring was continued for 2 h more. During this period, the orange material dissolved and concurrently a green microcrystalline product deposited. This was collected by filtration, and on recrystallization from acetonitrile−methanol (1:1) mixture bright green crystals were obtained; yield 0.51 g (35%). Anal. Calcd for $C_{25}H_{39}N_4O_{11}ClCuV$: C, 41.61; H, 5.41; N, 7.77. Found: C, 41.37; H, 5.51; N, 7.72. Selected IR data [ν, cm^{-1}]: 3280 w, 3260 w (νNH), 1610 w (δNH), 1550 s ($\nu_{as}CO_2^-$), 1415 s($\nu_sCO_2^-$), 1110 s, 630 m (νClO_4^-), 975 s (νV=O). UV−vis data [λ_{max}, nm (ϵ, M^{-1} cm^{-1})] in acetonitrile: 670 (75), 380 (690), 285 sh (8550). μ_{eff}: 2.60μ_B at 300 K.

Crystal Structure Determination of $[(V^{IV}O)L1Cu^{II}(\mu\text{-OAC})(MeOH)](ClO_4)$ (1). Crystals suitable for structure determination were obtained by slowly diffusing diethyl ether to a solution of **1** in acetonitrile−methanol (1:1) mixture.

Diffraction data were collected on a Siemens R3m/V diffractometer in the $\omega-2\theta$ scan mode at 293K using graphite-monochromatized Mo Kα radiation. Pertinent crystallographic data are summarized in Table 1. Three standard reflections were periodically monitored, and no crystal decay was observed. The intensity data were corrected for Lorentz and polarization effects, and semiempirical absorption correction was made from ψ scans. A total of 7424 reflections were collected in the range $2\theta = 3.8-55.3°$, with $-17 \le h \le 15$, $0 \le k \le 19$, and $0 \le l \le 22$, of which 7186 independent reflections ($R_{int} = 0.0404$) were used for structure determination. The structure was solved by direct and Fourier methods and refined by full-matrix least-squares methods based on F^2 using the programs SHELXTL-PLUS[25] and SHELXL-93.[26] Neutral atom scattering factors were taken from Cromer and Waber.[27] All non-hydrogen atoms, except the disordered perchlorate oxygen atoms, were refined anisotropically, while the disordered oxygens were refined isotropically. The hydrogen atoms were placed at the geometrically calculated positions with thermal parameters fixed at 1 plus the isotropic thermal parameters of the carbon atom to which each was bonded. The perchlorate anion is disordered over two sites with O(11) and Cl(1) at the same positions for both orientations, O(121)−O(141) have occupation factors of 0.287, while O(122)−O(142) have 0.713. The final least-squares refinement converged to $R1 = 0.063$ based on $F > 4\sigma(F)$, and w$R2 = 0.166$ based on all data. The final difference Fourier map was essentially featureless, the largest peak being 0.75 and the deepest hole −0.58 e $Å^{-3}$.

Results and Discussion

Synthesis and Characterization. A prerequisite for the synthesis of the heterobimetallic complexes of the symmetrical macrocyclic ligand H_2L1 is to use a suitable precursor complex in which one of the ligand compartments is vacant. Although such species is not readily obtainable for most of the metals, facile synthesis of $[VOL1]\cdot H_2O$[20b] by reacting $[VO(acac)_2]$ with H_2L1 provides a convenient starting material for the synthesis of $V^{IV}OM^{II}$ complexes. However, preliminary studies indicated that while almost insoluble $[VOL1]\cdot H_2O$ readily reacts with the perchlorate salts of the metal ions under consideration, the desired heterobinuclear complexes could not be isolated. On the contrary, the product obtained, for example, in the case of copper was $[Cu_2L1(ClO_4)_2]$.[24b] It became apparent that in order to produce thermodynamically stable heterobimetallic compounds it is necessary to obviate scrambling of the metallic sites, which was thought to be realized by providing an additional bridge between the metal centers. Indeed, when $[VOL1]\cdot H_2O$ is reacted with an equimolar amount of $M(ClO_4)_2\cdot 6H_2O$ (M = Cu, Ni, Co, Fe, Mn) in the presence of NaOAc, the products $[(VO)L1Cu(\mu\text{-OAC})(MeOH)](ClO_4)$ (**1**) and $[(VO)L1M(\mu\text{-OAC})(H_2O)](ClO_4)\cdot H_2O$ (**2**−**5**) are obtained in good yield. As reported earlier,[20a] unlike H_2L1, the reaction between $[VO(acac)_2]$ and H_2L2 produces a mixture of two forms of $[(V^{IV}O)L2]$ along with a small fraction of $[(V^{V}O(OH)L2]$. This mixture on treatment with $Cu(ClO_4)_2\cdot 6H_2O$ and NaOAc leads to the formation of $[(VO)L2Cu(\mu\text{-OAC})(H_2O)](ClO_4)\cdot H_2O$ (**6**) in 35% yield.

The characterization data of the complexes are given in the Experimental Section. The V=O stretching frequency for complexes **1**−**5** lies in the narrow range 935−950 cm^{-1}, while for **6** this band is shifted to a higher energy, 975 cm^{-1}. The difference in energy between $\nu_{as}CO_2^-$ and $\nu_sCO_2^-$ for all the complexes ranges from 135 to 165 cm^{-1}, which is typical of carboxylate-bridged compounds.[28] The other common IR spectral features of the complexes include bands due to the ligand NH stretching (3260 cm^{-1} for **1**−**5**, and 3280 and 3260 cm^{-1} for **6**) and bending (ca. 1610 cm^{-1}) and uncoordinated perchlorate anion (ca. 1100 and 630 cm^{-1}).

The absorption spectra of complexes **2**−**5** over the range 250−900 nm exhibit three bands with their peaks occurring at 730−715, 535−525, and 290−270 nm. Since for the $V^{IV}OMn^{II}$ complex (**5**) the spin-forbidden d−d transitions of the manganese(II) are likely to be too weak to be seen, the observed bands may therefore be reasonably attributed to $d_{xy} \rightarrow d_{yz}$, $d_{zx}(\nu_1)$, $d_{xy} \rightarrow d_{x^2-y^2}(\nu_2)$, and $d_{xy} \rightarrow d_{z^2}(\nu_3)$ transitions of the oxovanadium(IV) center with increasing order or energy. In complexes **2**−**4** shapes of the above-mentioned bands differ, however, presum-

(25) *SHELXTL-PLUS*; Siemens Crystallographic Research Systems; Madison, WI, 1990.
(26) Sheldrick, G. M. *SHELXL-93: A Program for Crystal Structure Refinement*; University of Göttingen: Göttingen, Germany, 1993.
(27) Cromer, D. T.; Waber, J. T. *International Tables for X-ray Crystallography*; The Kynoch Press: Birmingham, England, 1974; Vol. IV.
(28) Nakamoto, K. *Infrared and Raman Spectra of Inorganic and Coordination Compounds*, 3rd ed.; John Wiley: New York, 1978; p 232.

Table 2. Atomic Coordinates[a] ($\times 10^4$) and Equivalent Isotropic Displacement Parameters ($Å^2 \times 10^3$) of [($V^{IV}O$)L1Cu^{II}(μ-OAC)(MeOH)](ClO_4) (**1**)[a]

atom	*x*	*y*	*z*	*U*(eq)[b]	atom	*x*	*y*	*z*	*U*(eq)[b]
Cu(1)	8360(1)	1746(1)	7386(1)	44(1)	C(14)	9236(5)	3601(4)	7275(4)	58(2)
V(1)	7263(1)	287(1)	8056(1)	40(1)	C(15)	8684(5)	3307(4)	8458(4)	58(2)
O(1)	7859(3)	1532(2)	8382(2)	41(1)	C(16)	7444(4)	2181(4)	8741(3)	42(1)
O(2)	8177(3)	395(2)	7332(2)	42(1)	C(17)	7759(4)	3066(4)	8721(3)	49(1)
O(3)	6599(3)	2041(2)	6533(2)	49(1)	C(18)	7262(5)	3743(4)	9018(3)	52(1)
O(4)	8044(3)	−308(3)	8858(2)	61(1)	C(19)	6483(5)	3568(4)	9355(3)	49(1)
O(5)	5941(3)	864(2)	6997(2)	46(1)	C(20)	6250(5)	2693(4)	9433(3)	53(1)
N(1)	6061(3)	464(3)	8593(3)	44(1)	C(21)	6720(4)	1986(4)	9155(3)	45(1)
N(2)	6479(3)	−871(3)	7387(3)	44(1)	C(22)	6512(5)	1045(4)	9358(4)	54(1)
N(3)	8787(4)	1759(3)	6348(3)	51(1)	C(23)	8246(5)	−1905(5)	4650(4)	71(2)
N(4)	8477(4)	3085(3)	7563(3)	49(1)	C(24)	5937(5)	4321(4)	9644(4)	64(2)
C(1)	5590(5)	−363(4)	8813(4)	52(1)	C(25)	5836(4)	1567(3)	6556(3)	40(1)
C(2)	5072(5)	−947(4)	8047(4)	54(1)	C(26)	4682(4)	1819(4)	6010(4)	54(1)
C(3)	5881(5)	−1457(4)	7781(4)	54(1)	Cl(1)	2881(2)	4127(1)	3070(2)	82(1)
C(4)	7287(5)	−1439(4)	7202(4)	57(2)	O(11)	1950(4)	3617(4)	2753(4)	127(2)
C(5)	8189(4)	−166(4)	6700(3)	41(1)	O(121)*	3792(8)	3604(9)	3442(21)	186(7)
C(6)	7725(4)	−1015(4)	6584(4)	46(1)	O(131)*	2819(14)	4783(15)	3607(18)	112(3)
C(7)	7749(4)	−1555(4)	5916(4)	51(1)	O(141)*	2982(22)	4549(21)	2356(8)	211(7)
C(8)	8228(4)	−1292(4)	5367(3)	50(1)	O(122)**	3663(6)	3865(6)	2763(8)	112(3)
C(9)	8716(4)	−465(4)	5507(4)	51(1)	O(132)**	3335(11)	3884(10)	3955(4)	211(7)
C(10)	8717(4)	95(4)	6154(3)	45(1)	O(142)**	2748(7)	5020(4)	3025(10)	186(7)
C(11)	9375(5)	940(4)	6297(4)	55(2)	C(100)	10432(8)	954(7)	9159(7)	136(4)
C(12)	9398(5)	2526(4)	6188(4)	65(2)	O(100)	10241(4)	1599(4)	8420(3)	80(1)
C(13)	9020(6)	3414(4)	6356(4)	68(2)					

[a] Site occupancy: * = 0.287, ** = 0.713. [b] *U*(eq) is defined as one-third of the trace of the orthogonalized $\mathbf{U}_{ij}$ tensor.

ably due to superposition of d−d transitions of the second metal center. Additionally, complexes **2**−**4** each exhibit a characteristic band in the range 900−1200 nm. For the $V^{IV}ONi^{II}$ complex (**2**), the band observed at 1060 nm is evidently due to $^3A_{2g} \rightarrow {}^3T_{2g}$ transition of the nickel(II) center in an octahedral environment. Similarly, the bands occurring at 1000 (for **3**) and 1020 nm (for **4**) are attributable to $^4T_{1g} \rightarrow {}^4T_{2g}$ and $^5T_{1g} \rightarrow {}^5E_g$ transitions of octahedral cobalt(II) and iron(II), respectively.

The absorption spectra of the two $V^{IV}OCu^{II}$ complexes (**1** and **6**) show similar features with three peaks appearing at about 680, 385, and 290 nm. The very broad nature of the first band, spanning the range 450−900 nm, suggests that the d−d transitions due to the copper(II) and vanadium(IV) centers are not resolved in this range. The band at ca. 385 nm, which is not observed in the other complexes, is likely to be due to phenolate → copper(II) charge-transfer transition.[29] Taken together, the IR and electronic spectra suggest that the heterobinuclear complexes under consideration have similar stereochemical environment.

The electrochemical behavior of complexes **1**−**5** was studied by means of cyclic voltammetry and differential pulse voltammetry. For oxidation, an acetonitrile solution and a platinum electrode were used, while for reduction, a dimethyl sulfoxide solution and a glassy carbon electrode were used. Concerning the redox activity in the negative potential range 0 to −1 V, only the VOCu complex (**1**) undergoes quasireversible reduction at −0.61 V (ΔE_p = 100 mV at ν = 100 mV s^{-1}) due to Cu^{II}/Cu^{I}, while the other compounds lack electrochemical response in this range. At more negative potentials, complications arise due to demetalation reaction and consequent electrode poisoning. Complex **1**, on the other hand, is not electroactive in the positive potential range 0−1.5 V. In this range both VONi (**2**) and VOCo (**3**) undergo two successive irreversible electron-transfer reactions at ca. 1.0 and 1.2 V. For the VOMn complex (**5**), a quasireversible couple due to Mn^{II}/Mn^{III} occurs at 0.62 V (ΔE_p = 100 mV at ν = 100 mVs^{-1}), while the oxidation of $V^{IV}O$ to $V^{V}O$ takes place irreversibly at ca. 1.0 V. Again in the case of the VOFe complex (**4**), facile oxidation of the iron(II) center takes place nearly reversibly at 0.21 V (ΔE_p = 80 mV at ν = 100 mVs^{-1}).

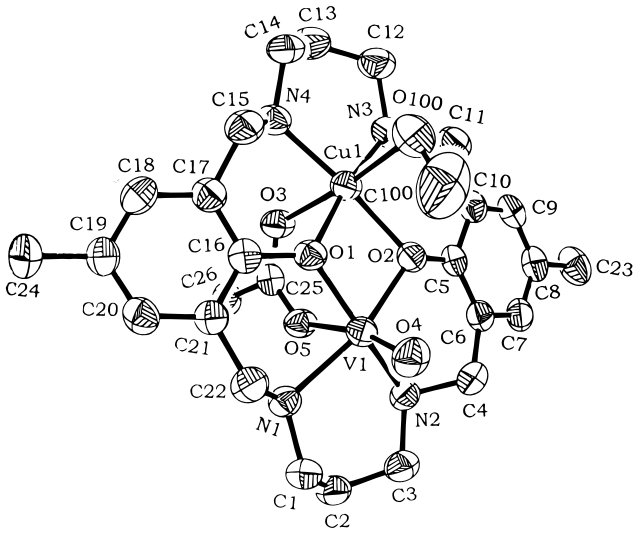

Figure 1. ORTEP representation of the structure of [($V^{IV}O$)L1Cu^{II}-(μ-OAC)(MeOH)]$^+$ cation in **1** showing the 50% probability thermal ellipsoids.

Structure of [($V^{IV}O$)L1Cu^{II}(μ-OAC)(MeOH)](ClO_4) (1). An ORTEP representation of the cation in **1** along with atom labels is shown in Figure 1. Atomic coordinates and selected bond distances and angles are given in Tables 2 and 3, respectively. Structure of **1** shows that the two metal centers are triply bridged by the two phenolate oxygens and the acetate ion. Both the metal centers are six-coordinated with distorted octahedral geometry and have N_2O_2 equatorial donors provided by the macrocyclic ligand. The remaining position of vanadium is occupied by the oxo oxygen (O(4)) and that of copper by distant contact with the methanol oxygen (O(100)). Although the copper center is only slightly displaced (0.019(1) Å) from its O(1)O(2)N(3)N(4) basal plane, the vanadium center is pushed

(29) Adhikary, B.; Mondal, S. K.; Nag, K. *J. Chem. Soc., Dalton Trans.* **1988**, 935.

toward O(4) by 0.258(1) Å from the O(1)O(2)N(1)N(2) equatorial plane. On the other hand, with reference to the best plane formed by the four secondary amine nitrogens, N(1)−N(4), the copper and vanadium atoms are displaced by 0.398(1) and 0.645(1) Å, respectively. As a result of the acetate bridging, the complex is distorted to such an extent that the dihedral angles between the equatorial planes of the metal centers is 32.0°, and that of the two phenyl rings is 29.3°. Moreover, the interplanar angle between Cu−O(1)−V and Cu−O(2)−V is 25.3°. The two metal centers are separated by 3.067 Å with two almost equal phenoxo bridge angles, 97.47(14) and 98.02(14)°.

The distorted geometry around vanadium is reflected in the transoid angles (164.2(2)−166.8(2)°) and cisoid angles (78.5(2)−104.2(2)°). The in-plane V−N distances (2.114(4) and 2.130(4) Å) and the V−O(phenolate) distances (2.013(4) and 2.034(3) Å) are normal, as is the axial V═O distance (1.627(4) Å). The V−O(acetate) distance, however, is significantly long (2.158(4) Å) due to the trans effect of the vanadyl group.

In the equatorial plane of the six-coordinated copper(II) center the two Cu−N distances (2.019(5) and 2.049(4) Å) and the two Cu−O(phenolate) distances (2.066(3) and 2.029(3) Å) are unexceptional. As compared to these, the axial Cu−O(MeOH) bond (2.452(2) Å) and Cu−O(OAc) bond (2.272(4) Å) are very long, signifying strong tetragonal distortion due to the Jahn−Teller effect.

As already mentioned, the perchlorate ion is disordered and has been modeled over two sites with unequal occupancies (0.287 and 0.713). No intramolecular hydrogen bonding is present in **1**. However, there is a fairly strong intermolecular interaction between the methanol OH and the O(11) atom of the ClO_4^- anion with O(100)···O(11) = 2.91(1) Å and O(100)−H···O(11) = 159.5°. An additional weak interaction is observed between one of the amines (N(1)) and a perchlorate oxygen with N(1)···O(122) = 3.11(1) Å and N(1)−H···O(122) = 145.7°.

Magnetism. The theoretical expressions for exchange coupling constants of the systems under consideration have been osbtained by using the HDvV Hamiltonian, $\mathbf{H} = -2J\mathbf{S}_1\cdot\mathbf{S}_2$. The effect of single-ion zero-field interaction ($D\mathbf{S}_z^2$), temperature-independent paramagnetism (TIP), mononuclear paramagnetic impurity (p), and the Weiss constant (θ) have been taken into consideration wherever required. In least-squares fittings of the experimental data to the theoretical expression, the residual $R = [\sum\{(\chi_M T)_{obs} - (\chi_M T)_{calc}\}^2/\sum(\chi_M T)_{obs}^2]$ has been minimized.

The spin-Hamiltonian for the $Cu^{II}V^{IV}O$ pair is given by

$$\mathbf{H} = -2J\mathbf{S}_{Cu}\cdot\mathbf{S}_{VO} + \beta(\mathbf{g}_{Cu}\mathbf{S}_{zCu} + \mathbf{g}_{VO}\mathbf{S}_{zVO})\cdot H \qquad (1)$$

which leads to the following expression[15] for χ_M

$$\chi_M = \frac{N\beta^2 g^2}{kT}\frac{2e^{2J/kT}}{1+3e^{2J/kT}} + \frac{N\beta^2\delta^2}{JT}\frac{e^{2J/kT}}{3e^{2J/kT}+1} \qquad (2)$$

$$\text{where} \qquad g = \frac{g_{Cu}+g_{VO}}{2}$$

$$\text{and} \qquad \delta = \frac{g_{Cu}-g_{VO}}{2}$$

The second term in eq 2 is due to second-order coupling of the two $M_s = 0$ components associated to the $S_T = 1$ and 0 levels, respectively. This term vanishes not only for equivalent metal centers but also its contribution is negligible for a $Cu^{II}V^{IV}O$ pair with appreciable singlet−triplet energy gap. Thus, taking into consideration the presence of single ion impurity and temperature-independent paramagnetism the working expression for χ_M becomes

$$\chi_M = \frac{N\beta^2 g^2}{kT}\frac{1+2e^{2J/kT}}{1+3e^{2J/kT}}(1-p) + \frac{N\beta^2 g^2 p}{4kT} + \text{TIP} \qquad (3)$$

For the $Ni^{II}V^{IV}O$ pair, neglecting local anisotropy and anisotropic interaction, eq 4 gives the theoretical expression for susceptibility

$$\chi_M = \frac{N\beta^2}{4kT}\frac{g_{1/2}{}^2 + 10g_{3/2}{}^2 e^{3J/kT}}{1+2e^{3J/kT}} + \text{TIP} \qquad (4)$$

where $g_{1/2}$ and $g_{3/2}$ are the g values of the pair states $S_T = {}^1/_2$ and ${}^3/_2$, respectively, which in turn are related to the local g values[30] as

$$g_{3/2} = \frac{2g_{Ni} + g_{VO}}{3}$$

$$g_{1/2} = \frac{4g_{Cu} - g_{VO}}{3}$$

It may be noted that although nickel(II) ion can have a substantial zero-field splitting, this effect has not been taken into consideration in the theoretical expression of χ_M (eq 4) to avoid overparametrization of the fitness parameters.

For the $Co^{II}V^{IV}O$ and $Fe^{II}V^{IV}O$ complexes the effect of single-ion zero-field interactions has been taken into consideration in the spin-Hamiltonian (eq 5).

$$\mathbf{H} = -2J\mathbf{S}_1\cdot\mathbf{S}_2 + D\mathbf{S}_z{}^2 \qquad (5)$$

The theoretical expression for magnetic susceptibility of $Co^{III}V^{IV}O$ (**3**) is given by eq 6. In this case it has been necessary to include the Weiss constant θ to obtain better fit.

$$\chi_M = \frac{2N\beta^2 g^2}{k(T-\theta)}\frac{e^A + 4e^C + e^E}{2e^A + e^B + e^D + e^E} + \text{TIP} \qquad (6)$$

where

$$A = [4J + 5/4D - (4J^2 - 2DJ + D^2)^{1/2}]/kT$$

$$B = [2J + {}^1/_4D]/kT$$

$$C = [6J + {}^9/_4D]/kT$$

$$D = [6J + {}^1/_4D]/kT$$

$$E = [(4J + {}^5/_4D) + (4J^2 - 2DJ + D^2)^{1/2}]/kT$$

Similarly, for $Fe^{II}V^{IV}O$ (**4**)

$$\chi_M = \frac{N\beta^2 g^2}{4kT}\frac{25e^A + 9e^B + e^C + 9e^D + e^E}{e^A + e^B + e^C + e^D + e^E} + \text{TIP} \qquad (7)$$

(30) (a) Chao, C. C. *J. Magn. Reson.* **1973**, *10*, 1. (b) Scaringe, R. P.; Hodgson, D. J.; Hatfield, W. E. *Mol. Phys.* **1978**, *35*, 701.

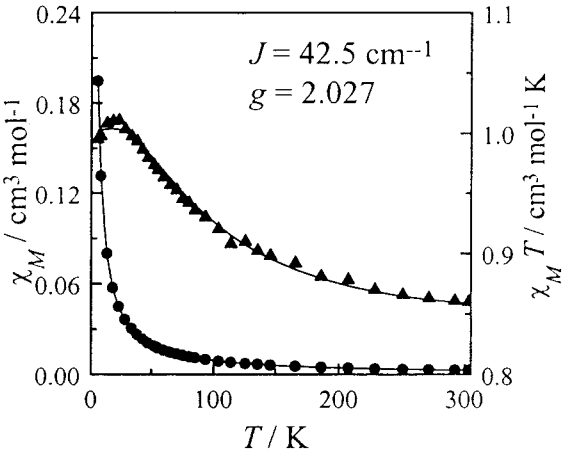

Figure 2. Plots of $\chi_M T$ and χ_M *vs* T for **1**. Solid lines represent the best least- squares fit of the experimental data to the theoretical equation.

where

$$A = [35/4J + 4D]/kT$$

$$B = [(25/4J + {}^5/_2D) + (25/4J^2 - {}^9/_2DJ + {}^9/_4D^2)^{1/2}]/kT$$

$$C = [(25/4J + {}^1/_2D) + (25/4J^2 - {}^1/_2DJ + {}^1/_4D^2)^{1/2}]/kT]$$

$$D = [(25/4J + {}^5/_2D) - (25/4J^2 - {}^9/_2DJ + {}^9/_4D^2]/kT]$$

$$E = [(25/4J + {}^1/_2D) - (25/4J^2 - {}^1/_2DJ + {}^1/_4D^2)^{1/2}]/kT$$

Finally, for the $Mn^{II}V^{IV}O$ complex (**5**) the following expression of χ_M has been used

$$\chi_M = \frac{N\beta^2}{k(T-\theta)} \frac{10g_2{}^2 + 28g_3{}^2\, e^{6J/kT}}{5 + 7e^{6J/kT}} + \text{TIP} \qquad (8)$$

where

$$g_3 = \frac{5g_{Mn} + g_{VO}}{6}$$

$$g_2 = \frac{7g_{Mn} - g_{VO}}{3}$$

The cryomagnetic behavior of the $Cu^{II}V^{IV}O$ complex, **1**, in the temperature range 4−300 K is shown in Figure 2 in the forms of $\chi_M T$ and χ_M vs T plots. As may be noted, on lowering of temperature from 300 to 12 K, $\chi_M T$ steadily increases and reaches a plateau between 22 and 12 K, then drecreases on further cooling. This behavior is typical of intradimer ferromagnetic exchange interaction. Satisfactory least-squares fitting of the experimental data to eq 3 can be obtained with $J = 42.5$ cm^{-1} and $g = 2.03$ (Table 4). The decrease of $\chi_M T$ below 12 K is most likely due to an intermolecular antiferromagnetic interaction between the $S_T = 1$ states.

Variable-temperature magnetic behavior of the other $Cu^{II}V^{IV}O$ complex, **6**, (shown in Figure 3) is very similar to that of **1**. In this case also the triplet state is populated below 22 K. The best fit curve is obtained with $J = 46.0$ cm^{-1} and $g = 2.01$.

The magnetic behavior of the acetate-bridged $Ni^{II}V^{IV}O$ complex (**2**), shown in Figure 4, is again indicative of ferromagnetic exchange interaction between the two metal centers. Least-squares fitting of the experimental data to eq 4 gives $J =$ 12.0 cm^{-1}, $g_{Ni} = 2.24$, and $g_{VO} = 1.97$. For this complex $\chi_M T$ reaches maximum at 12 K which is due to $S_T = {}^3/_2$ state with $g_{3/2} = 2.15$, indicating that at this temperature molecular doublet state ($S_T = {}^1/_2$) is totally depopulated. As may be noted in Figure 4, on further lowering of temperature, a rapid decrease of $\chi_M T$ occurs and in this region the best fit curve also deviates from the experimental data. This departure is most likely due to the zero-field splitting of the nickel(II) ion whose contribution has not been taken into consideration in eq 4.

Table 3. Selected Bond Distances (Å) and Angles (deg) of $[(V^{IV}O)L1Cu^{II}(\mu\text{-OAC})(MeOH)](ClO_4)$ (**1**)

Cu−N(4)	2.019(5)	V−N(1)	2.130(4)
Cu−N(3)	2.049(4)	V−N(2)	2.114(4)
Cu−O(1)	2.066(3)	V−O(1)	2.013(3)
Cu−O(2)	2.029(3)	V−O(2)	2.034(3)
Cu−O(3)	2.272(4)	V−O(5)	2.158(4)
Cu−O(100)	2.452(4)	V−O(4)	1.627(4)
Cu···V	3.066(1)		
N(3)−Cu−O(1)	171.3(2)	N(1)−V−O(2)	164.2(2)
N(4)−Cu−O(2)	172.7(2)	N(2)−V−O(1)	164.8(2)
O(100)−Cu−O(3)	172.3(13)	O(4)−V−O(5)	166.8(2)
O(3)−Cu−N(3)	89.9(2)	O(5)−V−N(1)	79.0(2)
O(3)−Cu−N(4)	84.5(2)	O(5)−V−N(2)	78.5(2)
O(3)−Cu−O(1)	89.08(13)	O(5)−V−O−(1)	88.31(14)
O(3)−Cu−O(2)	95.07(13)	O(5)−V−O(2)	86.65(14)
Cu−O(1)−V	97.47(14)	O(4)−V−N(1)	92.7(2)
Cu−O(2)−V	98.02(14)	O(4)−V−N(2)	91.8(2)
		O(4)−V−O(1)	102.4(2)
		O(4)−V−O(2)	102.6(2)

The $Co^{II}V^{IV}O$ complex (**3**) also exhibits ferromagnetic interaction. The μ_{eff} value at 298 K ($5.32\mu_B$), however, is much higher than the value ($4.24\mu_B$) expected for two uncoupled spins of $S_{Co} = {}^3/_2$ and $S_{VO} = {}^1/_2$. In this case $\chi_M T$ slowly increases with decrease of temperature reaching a maximum at 70 K and then slowly decreases up to 17 K, below which temperature the decrease is rapid. The observed magnetic behavior of **3** is rather complicated probably due to the unquenched orbital momentum of the cobalt(II) ion. Even after taking into account the single-ion zero-field interaction and the Weiss constant θ (eq 6) only a moderate fit ($R = 1.2 \times 10^{-2}$) could be obtained with $J = 4.4$ cm^{-1}, $g = 2.53$, $|D| = 0.2$ cm^{-1}, and $\theta = -3.1$ K.

As shown in Figure 5, the $Fe^{II}V^{IV}O$ complex (**4**) is also ferromagnetically coupled. The μ_{eff} value at 298 K is $5.70\mu_B$, which slowly increases on lowering of the temperature until a plateau is reached in the temperature range 22−12 K with $\mu_{eff} = 6.0\mu_B$. Below 12 K, there is a decrease in μ_{eff} reaching a value of $5.54\mu_B$ at 5 K, presumably due to the zero-field effect of the high-spin iron(II) ion ($S_{Fe} = 2$). Least-squares fitting of the experimental data to eq 7 gives $J = 4.4$ cm^{-1}, $g = 2.18$, and $|D| = 0.75$ cm^{-1}.

The cryomagnetic behavior of the $Mn^{II}V^{IV}O$ complex (**5**), shown in Figure 6, depicts a slow decrease of the $\chi_M T$ value on lowering the temperature from 300 to 90 K. The slope gets steeper in the range 90−30 K, below which almost a plateau is reached which again shows the sign of rapid decline below 8 K. The observed behavior is characteristic of an antiferromagnetically coupled system. An excellent fit of the experimental data to eq 8 has been obtained with $J = -14.2$ cm^{-1}, $g_{Mn} =$ 2.00, $g_{VO} = 1.86$, and $\theta = -0.68$ K. The total spin states for this system ($S_{Mn} = {}^5/_2$ and $S_{VO} = {}^1/_2$) are $S_T = 3$ and 2 with the g values $g_3 = 1.97$ and $g_2 = 2.02$. The value of μ_{eff} at the plateau ($4.87\mu_B$) is very close to the expected value ($4.94\mu_B$) for the $S_T = 2$ state with $g_2 = 2.02$.

The ferromagnetic behavior of the two $Cu^{II}V^{IV}O$ complexes (**1** and **6**) with their triplet−singlet energy gaps ($2J$) of 85 cm^{-1} (for **1**) and 92 cm^{-1} (for **6**) are quite similar to that of

Table 4. Magnetic Data for the Complexes

complex	J, cm^{-1}	g_{vo}	g_M	g_{av}	θ, K	D, cm^{-1}	p, %	10^6 TIP
1	42.5			2.027			4	120
2	12.0	1.97	2.24					160
3	4.4			2.53	−3.1	0.20		60
4	4.4			2.18		0.75		60
5	−14.2	1.86	2.00		−0.68			60
6	46.0			2.013			3	120

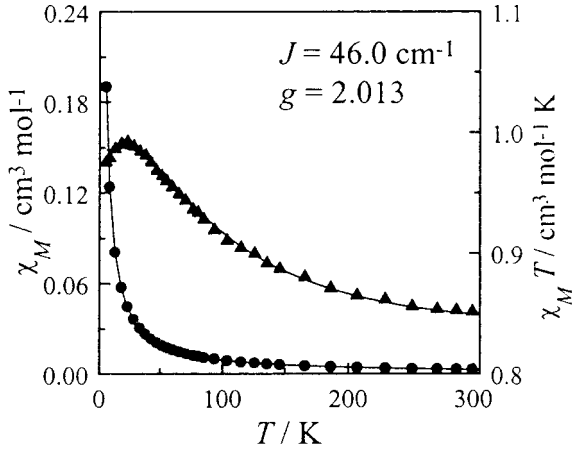

Figure 3. Plots of $\chi_M T$ and χ_M *vs* T for **6**. Solid lines represent the best least- squares fit of the experimental data to the theoretical equation.

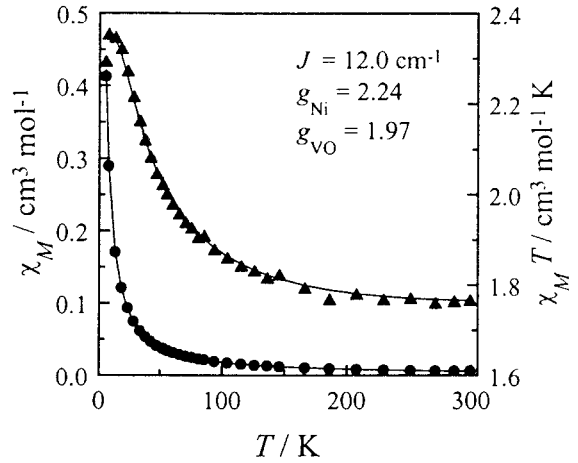

Figure 4. Plots of $\chi_M T$ and χ_M *vs* T for **2**. Solid lines represent the best least- squares fit of the experimental data to the theoretical equation.

$[Cu^{II}V^{IV}O\{(fsa)_2\text{-en}\}(CH_3OH)]$ (**7**) for which $2J = 118$ cm^{-1}.[15] As already noted from the crystal structure of **1**, the molecular symmetry of the compound can be approximated as C_s. The magnetic orbital on the copper(II) center, $d_{x^2-y^2}$, is roughly parallel to the copper-donor directions in the basal plane and engaged in σ overlap with the bridging phenolate oxygens, and transforms as a' irreducible representation of the C_s group. On the other hand, the magnetic orbital on vanadium(IV), d_{xy}, which roughly bisects all the equatorial cis angles, is delocalized toward the phenolate oxygens by π-type overlap and transforms as a'' irreducible representation of the C_s group. Thus, for the magnetic orbitals (ϕ_{Cu}, ϕ_{VO}) being symmetry-related orthogonal, there is essentially zero overlap ($<\phi_{Cu}|\phi_{VO}> \approx 0$), and no chemical bonding. This implies that in the expression of singlet−triplet energy gap $2J = J_{AF} + J_F$, the contribution of J_{AF} is insignificant.

It is of interest at this stage to compare the magnitude of exchange coupling constants of **1** and **7** vis-à-vis their structural parameters. Unlike **1**, in which both the metal centers are six-coordinated, in **7** each of the metal ions have square pyramidal

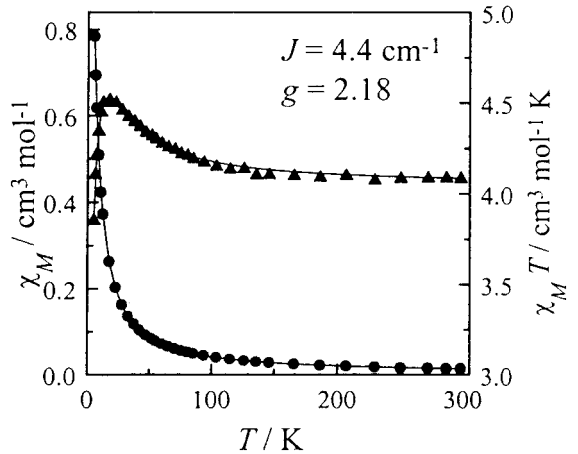

Figure 5. Plots of $\chi_M T$ and χ_M *vs* T for **4**. Solid lines represent the best least- squares fit of the experimental data to the theoretical equation.

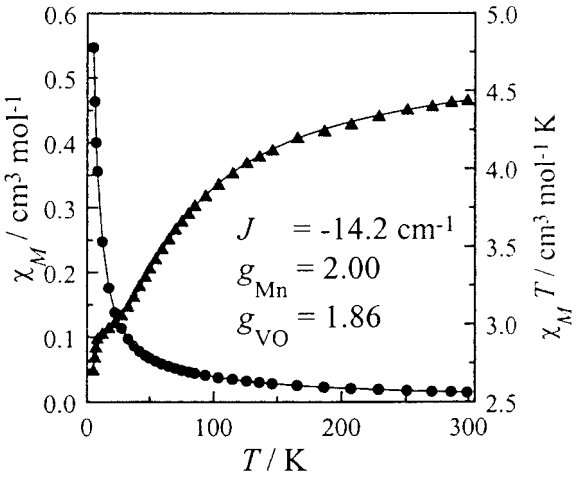

Figure 6. Plots of $\chi_M T$ and χ_M *vs* T for **5**. Solid lines represent the best least- squares fit of the experimental data to the theoretical equation.

geometry with syn configuration,[15] albeit the two compounds have C_s symmetry. A comparison of the Cu−O(phenoxo)−V bridge angles in **1** (97.5 and 98.0°) and **7** (98.4 and 98.9°) reveals that despite these angles being almost identical, the J values of the two compounds are quite different. This contrasts the observation of linear dependence of J on M−O−M bridge angle in the homobinuclear hydroxo-bridged copper(II)[8a] and phenoxo-bridged nickel(II)[9a] complexes. It should be noted, however, that the Cu···V separation in **7** (2.989(4) Å) is shorter relative to that in **1** (3.066(11) Å). Of greater relevance is the factor that can be expected to control the extent of ferromagnetic coupling in $Cu^{II}V^{IV}O$ complexes is the dihedral angle (Δ) between the equatorial planes of the two metal centers. On the basis of orbital overlap model, ferromagnetic exchange should be maximum when the two metal centers are exactly coplanar, i.e., $\Delta = 0°$. Conversly, J_F will be vanishingly small when the dihedral angle between the two metal planes is 90°. This explains why **7** with a lesser dihedral angle ($\Delta = 10.3°$) exhibits a stronger ferromagnetic interaction ($J = 59$ cm^{-1}) relative to

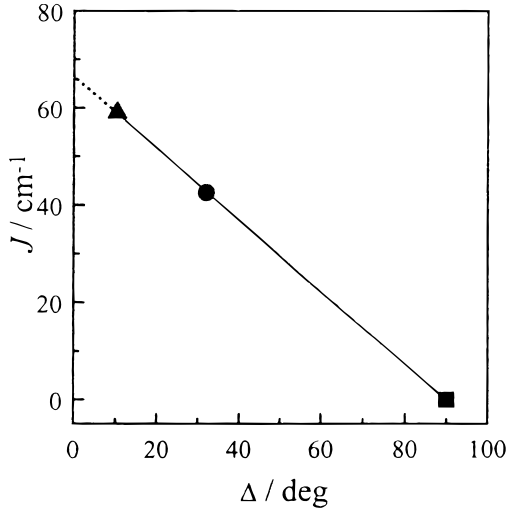

Figure 7. Plot of exchange coupling constant J vs dihedral angle Δ between the planes of the metal centers in **2** (●) and **7** (▲). The best fit line is obtained by considering $J = 0$ at $\Delta = 90°$ (■).

1 ($J = 42.5$ cm^{-1}) having a greater angle ($\Delta = 32.0°$). As shown in Figure 7, taking $J = 0$ at $\Delta = 90°$ as a boundary condition, an excellent linear fit is obtained for the J vs Δ plot of these two compounds. On the basis of this plot it may be anticipated that for a perfectly coplanar $Cu^{II}V^{IV}O$ complex, which, of course, is unlikely to be obtained, the separation between the triplet and singlet states will be as large as 133.5 cm^{-1}. The validity of the above J vs Δ correlation is borne out by the fact that the two compounds **1** and **7** differ not only structurally, but also the coordination environment of their metal centers differ (CuN_2O_4 and VN_2O_4 in **1** as against CuN_2O_3 and VO_5 in **7**). Clearly, to consolidate this magnetostructural relationship more data is needed. To our knowledge, only three more structurally characterized $Cu^{II}V^{IV}O$ complexes have been studied so far. Gatteschi et al.[31] have reported the magnetic properties of a phenoxo-bridged trinuclear $Cu_2^{II}V^{IV}O$ complex in which there is a strong ferromagnetic exchange coupling between the vanadium(IV) and one of the copper(II) centers. However, due to complex nature of interactions of the three metal centers the exchange integrals have been approximated as $J_{Cu(1)-V} = 0 \pm 5$ cm^{-1} and $J_{Cu(2)-V} = 42.5 \pm 0.5$ cm^{-1}. Kahn et al.[32] and Rojo et al.[33] have studied two oxalato-bridged $Cu^{II}V^{IV}O$ complexes. In both the cases, notwithstanding orthogonality of the magnetic orbitals, the overlap density ($\rho = \int \phi_{Cu}\phi_{VO}$) does not present any zone of strong magnitude and hence results in very weak ferromagnetic interaction.

The $Ni^{II}V^{IV}O$ complex (**2**) also exhibits ferromagnetic exchange interaction, but the magnitude of J (12.0 cm^{-1}) is considerably less than that of **2** (42.5 cm^{-1}). In high-spin nickel(II) the unpaired electrons are in the e_g state, i.e., $d_{x^2-y^2}$ and d_{z^2} represent the magnetic orbitals. Assuming that the structures of **1** and **2** are related, the σ/π symmetry mismatch is retained for $d_{xy} \leftrightarrow d_{x^2-y^2}$ interaction in the $Ni^{II}V^{IV}O$ complex and providing a pathway for ferromagnetic exchange coupling. By contrast, the d_{xy} orbital of $V^{IV}O$ and the d_{z^2} orbital of Ni^{II} both transform to the same irreducible representation a' of the group C_s, thus giving rise to antiferromagnetic interaction. Clearly, the ferromagnetic interaction prevails over the antiferromagnetic interaction. In a previous study,[20b] we reported the magnetic properties of two more $Ni^{II}V^{IV}O$ complexes of the same macrocyclic ligand, viz., $[(V^{IV}O)L1Ni^{II}(\mu\text{-}SO_4)(H_2O)]0\cdot 2H_2O$ and $[(V^{IV}O)L1Ni^{II}(SO_4)(H_2O_2)]\cdot H_2O$ for which the J values are 6 and 10 cm^{-1}, respectively. Thus, all the three $Ni^{II}V^{IV}O$ complexes exhibit overall ferromagnetic effect and the small difference in J values may reflect differences in the angles between the metal planes.

The ferromagnetic behavior of the $Co^{II}V^{IV}O$ complex ($J = 4.4$ cm^{-1}) is expected. For the $Fe^{II}V^{IV}O$ complex (**4**), the pathways involving $d_{x^2-y^2} \leftrightarrow d_{xy}$, $d_{z^2} \leftrightarrow d_{xy}$, and $d_{zx} \leftrightarrow d_{xy}$ are expected to be ferromagnetic, weakly antiferromagnetic, and weakly ferromagnetic, respectively. A value of $J = 4.4$ cm^{-1}, as expected, indicates the dominating influence of $d_{x^2-y^2} \leftrightarrow d_{xy}$ interaction on the overall ferromagnetic behavior of the compound. However, the lower J value of **4** compared to that of **2** is not clear at this stage.

Finally, in the $Mn^{II}V^{IV}O$ complex (**5**) the two major interaction paths involve $d_{xy} \leftrightarrow d_{x^2-y^2}$ and $d_{xy} \leftrightarrow d_{xy}$, of which the former is ferromagnetic, while the latter is antiferromagnetic due to significant chemical bonding. Expectedly, the antiferromagnetic interaction is more prominent in this case ($J = -14.2$ cm^{-1}). It may be mentioned that substantial antiferromagnetic exchange coupling ($d_{xy} \leftrightarrow d_{xy}$) occurs in the related dioxovanadium(IV) complex $\{(VO)_2L1(\mu\text{-}SO_4)\}\cdot MeOH\cdot 3H_2O$,[21d] for which $J = -128$ cm^{-1}. For the sake of completion we note that the dicopper(II) complex $[Cu_2L1(ClO_4)_2]$ exhibits very strong antiferromagnetic exchange with the singlet−triplet energy gap of 824 cm^{-1}.[34]

To conclude, a comprehensive study has been made on the magnetic properties of a series of triply bridged $M^{II}V^{IV}O$ (M = Cu, Ni, Co, Fe, Mn) complexes of the macrocyclic ligand H_2L1. Except for the $Mn^{II}V^{IV}O$ complex, which is antiferromagnetically coupled, other complexes behave ferromagnetically. The magnitude of J in the symmetry-related interaction between the orthogonal magnetic orbitals $d_{xy} \leftrightarrow d_{x^2-y^2}$ of the $Cu^{II}V^{IV}O$ complex ($J = 42.5$ cm^{-1}) is influenced by the dihedral angle Δ between the planes of the two metal centers ($\Delta = 32.0°$). A linear dependence of J on Δ is proposed.

Acknowledgment. K.N. thanks the Department of Science and Technology, Government of India, for financial support.

Supporting Information Available: Tables of crystal data and intensity measurements, thermal parameters and hydrogen atom coordinates, and complete bond lengths and angles (6 pages). Ordering information is given on any current masthead page.

IC971176D

(31) Bencini, A.; Benelli, C.; Dei, A.; Gatteschi, D. *Inorg. Chem.* **1985**, *24*, 695.
(32) Julve, M.; Verdaguer, M.; Charlot, M. F.; Kahn, O. *Inorg. Chim. Acta* **1984**, *82*, 5.
(33) Cortes, R.; Urtiaga, M. K.; Lazama, L.; Arriortua, M. I.; Rojo, T. *Inorg. Chem.* **1994**, *33*, 829.
(34) Mandal, S. K.; Thompson, L. K.; Nag, K.; Charland, J. P.; Gabe, E. J. *Can. J. Chem.* **1987**, *65*, 2815.